Two-color photoassociation spectroscopy of ytterbium atoms and the precise determinations of *s*-wave scattering lengths

Masaaki Kitagawa,[1] Katsunari Enomoto,[1] Kentaro Kasa,[1] Yoshiro Takahashi,[1,2] Roman Ciuryło,[3] Pascal Naidon,[4] and Paul S. Julienne[4,5]

[1]*Department of Physics, Graduate School of Science, Kyoto University, Kyoto 606-8502, Japan*

[2]*CREST, Japan Science and Technology Agency, Kawaguchi, Saitama 332-0012, Japan*

[3]*Instytut Fizyki, Uniwersytet Mikołaja Kopernika, ul. Grudziędzka 5/7, 87–100 Toruń, Poland*

[4]*Atomic Physics Division, National Institute of Standards and Technology, 100 Bureau Drive, Stop 8423, Gaithersburg, Maryland 20899-8423, USA*

[5]*Joint Quantum Institute, National Institute of Standards and Technology, 100 Bureau Drive, Stop 8423, Gaithersburg, Maryland 20899-8423, USA*

(Received 3 August 2007; published 28 January 2008)

By performing high-resolution two-color photoassociation spectroscopy, we have successfully determined the binding energies of several of the last bound states of the homonuclear dimers of six different isotopes of ytterbium. These spectroscopic data are in excellent agreement with theoretical calculations based on a simple model potential, which very precisely predicts the *s*-wave scattering lengths of all 28 pairs of the seven stable isotopes. The *s*-wave scattering lengths for collision of two atoms of the same isotopic species are 13.33(18) nm for ^{168}Yb, 3.38(11) nm for ^{170}Yb, −0.15(19) nm for ^{171}Yb, −31.7(3.4) nm for ^{172}Yb, 10.55(11) nm for ^{173}Yb, 5.55(8) nm for ^{174}Yb, and −1.28(23) nm for ^{176}Yb. The coefficient of the lead term of the long-range van der Waals potential of the Yb_2 molecule is $C_6=1932(30)$ atomic units ($E_h a_0^6 \approx 9.573\times 10^{-26}$ J nm^6).

DOI: 10.1103/PhysRevA.77.012719 PACS number(s): 34.50.−s, 34.20.Cf, 37.10.De, 34.10.+x

I. INTRODUCTION

A collision between two atoms is a fundamental physical process and can be described by a few partial scattering waves for ultracold atoms. At a sufficiently low temperature the kinetic energy of colliding atoms becomes less than the centrifugal barrier, and only the *s*-wave scattering is possible. The *s*-wave scattering length is an essential parameter for describing ultracold collisions. It also governs the static and dynamic properties of quantum degenerate gases like a Bose-Einstein condensate (BEC) or a degenerate Fermi gas (DFG) of fermionic atoms in different spin states. Since the *s*-wave scattering length is very sensitive to the ground state interatomic potential, especially at short internuclear distance, the precise *ab initio* calculation of the scattering length is very difficult, and therefore we must resort to experimental determination. The most powerful approach for determining the scattering length is to measure the binding energy (E_b) of the last few bound states in the molecular ground state, since the energy E_b is closely related to the *s*-wave scattering length. So far, the binding energies were measured via two-color photoassociation (PA) spectroscopy for Li [1], Na [2], K [3], Rb [4], Cs [5], and He [6]. A schematic description is shown in Fig. 1. If a laser field L_2 is resonant to a bound-bound transition, it causes an Autler-Townes doublet. This effect is detected as a reduction of a rate of a free-bound PA transition driven by the other laser field L_1. This scheme is called Autler-Townes spectroscopy, and it is also explained in terms of the formation of a dark state. If both lasers are off-resonant and the frequency difference matches E_b, these lasers drive a stimulated Raman transition from the colliding atom pair to a molecular state in the electronic ground state. In this Raman spectroscopy, the resonance is detected as an atom loss.

The *s*-wave scattering length of two colliding atoms is determined by the adiabatic Born-Oppenheimer interaction potential $V(r)$ between the two atoms, which is very well approximated at large interatomic separation r by the van der Waals contribution, $V(r)\approx -C_6/r^6$, where C_6 is the van der Waals coefficient due to the dipole-dipole interaction. The *s*-wave scattering length is given by the following formula, based on a quantum correction to the WKB approximation so as to be accurate for the zero-energy ($E=0$) limit [7–9],

$$a=\bar{a}\left[1-\tan\left(\Phi-\frac{\pi}{8}\right)\right]. \quad (1)$$

Here $\bar{a}=2^{-3/2}[\Gamma(3/4)/\Gamma(5/4)](2\mu C_6/\hbar^2)^{1/4}$ is a characteristic length associated with the van der Waals potential, where

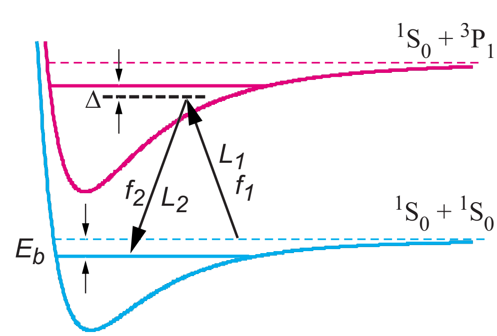

FIG. 1. (Color online) Schematic description of the two-color PA spectroscopy. The laser L_1 drives the one-color PA transition. The laser L_2 couples the bound state in the excited molecular potential to the one in the ground molecular potential. The detuning Δ of the PA laser with respect to the one-color PA resonance is set to several MHz for the Raman spectroscopy, while Δ is set to zero for the Autler-Townes spectroscopy.

Γ is the gamma-function, μ is the reduced mass, and $\hbar$ is the Planck constant divided by 2π. The semiclassical phase Φ is defined by

$$\Phi = \frac{\sqrt{2\mu}}{\hbar}\int_{r_0}^{\infty} \sqrt{-V(r)}dr, \tag{2}$$

where r_0 is the inner classical turning point of $V(r)$ at zero energy. The number of bound states N in the potential is [8]

$$N = \left[\frac{\Phi}{\pi} - \frac{5}{8}\right] + 1, \tag{3}$$

where the brackets mean the integer part. As was mentioned above, the scattering length is very sensitive to the phase Φ and can take on any value between $\pm\infty$ when Φ varies over a range spanning π. While the accurate calculation of Φ is very difficult since it requires a knowledge of the whole potential, Φ is proportional to $\sqrt{\mu}$, and so the formula in Eq. (1) gives a simple mass scaling of the isotopic variation of the scattering length once a and N are known for one isotopic combination. Mass scaling applies as long as small mass-dependent corrections to the Born-Oppenheimer potential [12–14] can be ignored. While mass scaling is often used for bound and scattering states for cold atomic systems [10,11], and seems applicable to large-mass systems within experimental uncertainties [15], exceptions are known [16], and its accuracy should be carefully tested for different kinds of systems.

Ytterbium (Yb) is a rare-earth element with an electronic structure similar to that of the alkaline-earth atoms. One of the unique features of Yb atoms is a rich variety of isotopes with five spinless bosons (^{168}Yb, ^{170}Yb, ^{172}Yb, ^{174}Yb, and ^{176}Yb) and two fermions (^{171}Yb with the nuclear spin $I=1/2$ and ^{173}Yb with $I=5/2$), which enables us to study various mixtures of degenerate gases of Yb atoms. In fact, recently, a BEC [17] and a DFG [18] of Yb atoms have been achieved. Another distinct feature of Yb atoms is the simple electronic ground state of $^1S_0$ symmetry. Therefore, the ground molecular state of Yb has only one potential of $^1\Sigma_g$ molecular symmetry with no electronic orbital and spin angular momenta. This is in contrast to the case of an alkali dimer which has spin-singlet $^1\Sigma_g$ and spin-triplet $^3\Sigma_g$ ground states with a complicated hyperfine structure. These two unique features of the Yb system, that is, the existence of a rich variety of isotopes and one simple isotope-independent molecular potential, offers the possibility to systematically check the scattering length theory with an unprecedented precision. If we can be confident in the theory, then it would enable us to determine the scattering lengths of all possible isotope pairs which are not measured experimentally. So far, to determine the s-wave scattering length of ^{174}Yb, one-color PA spectroscopy was performed [19], which gave the result of 5.53(11) nm. From the cross-dimensional rethermalization technique, the absolute value of the scattering length for ^{173}Yb was estimated as 6(2) nm [18], assuming that the spin was completely unpolarized. From the expansion of a condensate, the value of the scattering length for ^{170}Yb was estimated as 3.6(0.9) nm [20]. However, these values are not enough for a rigorous test of the theory.

In this paper, we report an accurate determination of the s-wave scattering lengths for all Yb isotopes including those for different isotope pairs. By using two-color PA spectroscopy with the intercombination transition $^1S_0-{}^3P_1$, we successfully determined the binding energy E_b of twelve bound states near the dissociation limit of four homonuclear dimers comprised of bosonic atoms (^{170}Yb$_2$, ^{172}Yb$_2$, ^{174}Yb$_2$, and ^{176}Yb$_2$) and two dimers comprised of fermionic atoms (^{171}Yb$_2$ and ^{173}Yb$_2$). The spectroscopically measured binding energies are in excellent agreement with theoretical calculations based on a simple model potential that was fit to the data. The calculated s-wave scattering lengths for the six isotopes obey the mass-scaling law with very good precision. Moreover, this excellent agreement allows us to accurately determine the scattering lengths of all twenty-eight different isotopic combinations. In addition, we can reveal scattering properties of other partial waves such as p- and d-wave scatterings and energy dependence of the elastic cross sections. These results are an important foundation for future research, such as the efficiency of evaporative cooling, stability of quantum gases and their mixtures, and the collision shifts of lattice clocks [21].

II. EXPERIMENT

The experimental setup was almost the same as our previous experiment of one-color PA spectroscopy [22]. All the experiments were performed at about 1 μK, where only the s-wave scattering is significant. Atoms were first collected in a magneto-optical trap (MOT) with the intercombination transition $^1S_0-{}^3P_1$ at 556 nm. The linewidth and saturation intensity of the transition were 182 kHz and 0.14 mW/cm^2, respectively. The laser beam for the MOT was generated by a dye laser whose linewidth was narrowed to less than 100 kHz. The dye laser was stabilized by an ultralow expansion cavity, whose frequency drift was typically less than 20 Hz/s. The number, density, and temperature of atoms in the MOT were about 2×10^7, 10^{11} cm^{-3}, and 40 μK, respectively. Then the atoms were transferred into a crossed far-off resonant trap (FORT). The number, density, and temperature of atoms in the FORT were about 2×10^6, 10^{13} cm^{-3}, and 100 μK, respectively. To reach lower temperatures, evaporative cooling was carried out by gradually decreasing the potential depth of the horizontal FORT beam to several tens of μK in several seconds. Evaporative cooling worked rather well for the bosonic isotopes, ^{170}Yb, ^{172}Yb, and ^{174}Yb, and for the fermionic isotope ^{173}Yb. Typically 1×10^5 atoms at the temperature of about 1 μK finally remained in the trap and the density was between 10^{13} cm^{-3} and 10^{14} cm^{-3}, although optimized evaporation ramps and efficiency for each isotope were different. In particular, we observed rapid atom decay for ^{172}Yb due to three-body recombination. The steeper evaporation ramp was needed for ^{172}Yb to obtain enough number of atoms. It is also noted that an unpolarized sample of ^{173}Yb enabled us to perform efficient evaporative cooling even at a low temperature via elastic collisions between atoms with different spins. For the bosonic ^{176}Yb and fermionic ^{171}Yb isotopes, however, the evaporative cooling did not work well. In order to cool ^{171}Yb and ^{176}Yb, we per-

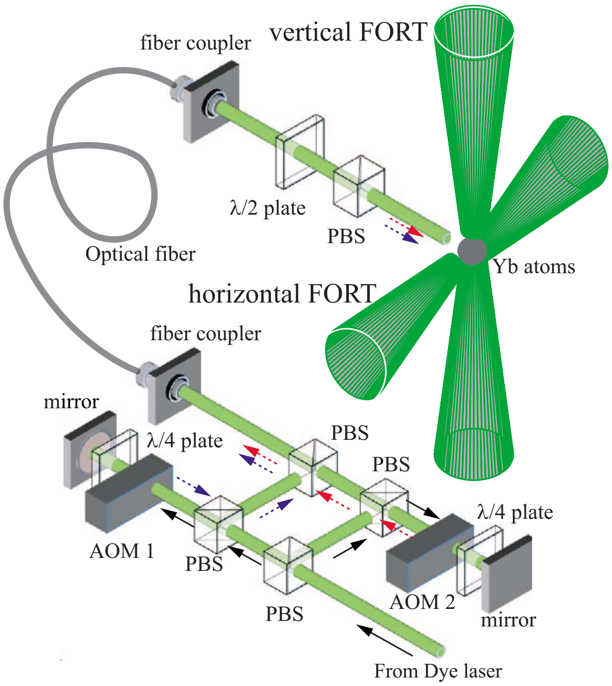

FIG. 2. (Color online) Schematic description of an experimental setup for PA lasers. The two lasers were prepared by splitting one laser, and two double-pass acousto-optic modulators (AOMs) were employed to tune them. Then the two lasers were aligned in the same path. The solid lines and broken lines indicate the laser beams before and after the double pass, respectively. A polarizing beam splitter (PBS) and a $\lambda/2$ plate after the optical fiber were employed to fix polarization of both lasers in the same direction.

formed sympathetic cooling with bosonic ^{174}Yb [23,24]. Bichromatic MOT beams for simultaneous trapping of two isotopes in the MOT were generated by an electro-optic modulator (EOM), of which the modulation frequency corresponds to the isotope shift. Typically 6×10^4 atoms for ^{171}Yb and 2×10^5 atoms for ^{176}Yb at the temperature of about 1 μK finally remained in the trap. The bosonic isotope of ^{168}Yb was hard to collect in the MOT due to its small natural abundance of 0.13%, although there are no fundamental difficulties for ^{168}Yb in principle.

After the evaporative cooling, the two lasers, L_1 for the free-bound transition and L_2 for the bound-bound transition, were simultaneously applied to the atoms in the trap for about 30 ms. These beams were focused to a 100 μm diameter. The schematic setup for the PA lasers is represented in Fig. 2. The two laser beams were prepared by splitting one laser beam for the MOT and therefore had the same frequency linewidth and stability as the MOT beam. The relative frequency was controlled by acousto-optic modulators (AOMs). The two laser beams were coupled in the same optical fiber. A polarizing beam splitter (PBS) and a half-wave ($\lambda/2$) plate after the optical fiber were inserted to fix the polarization of both lasers in the same direction. Finally, the PA laser beams were aligned to pass through the atoms in the FORT by using a CCD camera for absorption imaging. The detuning of the PA laser with respect to the atomic resonance $^1S_0-{}^3P_1$ was easily checked by observing the frequency at which the atoms in the MOT disappeared. The

TABLE I. Excited state rovibrational Yb dimer levels used for the free-bound PA transition, where v_e and J_e are the respective vibrational and rotational quantum numbers; v_e is numbered from the dissociation limit. The position of the excited state level is given as detuning in MHz from the frequency of the atomic $^1S_0-{}^3P_1$ transition. For the fermionic isotopes the hyperfine level with the largest total atomic angular momentum for the $^3P_1$ state defines the dissociation limit.

Isotope	v_e	J_e	Position (MHz)
^{170}Yb	16	1	618
^{171}Yb	[a]	[a]	904
^{172}Yb	17	1	789
^{173}Yb			791
^{174}Yb	18	1	993
	19	1	1972
^{176}Yb	17	1	868

[a]Reference [25].

power of the PA laser was monitored by a photodiode. For the Raman spectroscopy, the frequency f_1 of L_1 was fixed with a certain detuning Δ from a particular PA resonance, and the frequency f_2 of L_2 was scanned to search for the bound states of the ground state. For the Autler-Townes spectroscopy, f_1 was fixed to a particular PA resonance, and f_2 was scanned. Table I shows the excited state rovibrational levels used for the free-bound transition, where the resonance position is given in frequency detuning from the atomic $^1S_0-{}^3P_1$ transition. Our setup for the PA laser beams could provide enough power for detuning smaller than 1 GHz. To obtain enough power for detuning larger than 1 GHz, the sideband of the EOM was used for the MOT while the carrier is used as the PA lasers. We observed the two-color PA signals by measuring the number of surviving atoms with the absorption imaging method with the $^1S_0-{}^1P_1$ transition.

III. EXPERIMENTAL RESULTS

All the two-color PA spectra observed are shown in Fig. 3, where v is the vibrational quantum number counting down from the dissociation limit and J is the rotational quantum number. The observed spectral linewidth is typically several tens of kHz due to the finite energy distribution at the 1 μK temperature and the power broadening. The selection rule for the parity determines the observable quantum number J in the ground state $^1\Sigma_g^+$ as $0,2,4,\ldots$ from the s-wave collision. We observed all resonance positions with detuning less than 300 MHz from the dissociation limit except for the $v=2$ state for ^{173}Yb; see Fig. 6(b).

The observed peak positions included the light shift. We measured the peak positions with several laser intensities for L_1 and L_2 and different detunings Δ, in order to compensate the light shift by interpolation or extrapolation. We found that the bound-bound coupling is dominant for the light shift for the Raman spectroscopy. Namely, the light shift is expressed as

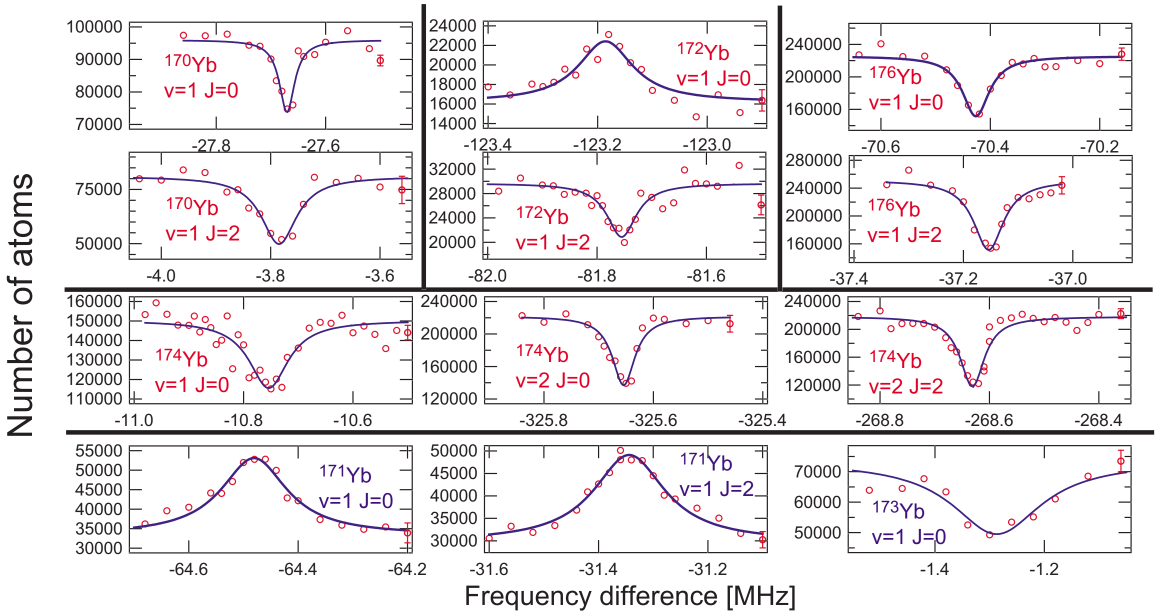

FIG. 3. (Color online) Two-color PA spectra at about 1 μK. The horizontal and vertical axes are the frequency difference between the two lasers and the number of remaining atoms, respectively. The vertical error bars represent the fluctuations of the number of atoms. The solid lines are fits of the Lorentz functions. The Autler-Townes spectroscopy is applied to the $v=1$, $J=0,2$ states of $^{171}\mathrm{Yb}_2$ and the $v=1$, $J=0$ state of $^{172}\mathrm{Yb}_2$, while the Raman spectroscopy is applied to the others.

$$\delta_{\mathrm{LS}} = \beta\left(\frac{I_1}{\Delta + f_1 - f_2} + \frac{I_2}{\Delta}\right), \tag{4}$$

where β is a constant related to the Franck-Condon factor of the bound-bound transition and I_1 and I_2 are the laser intensities of L_1 and L_2, respectively. Typical values of the detuning Δ and laser intensity were about 2 MHz and 10–1000 mW/cm^2. The contributions of the other excited bound states were negligible, since their resonance frequencies were typically more than 300 MHz apart, which was much larger than Δ and $\Delta+f_1-f_2$. Figure 4 shows the light shift δ_{LS} with several intensities for L_1 and L_2 and detuning Δ. The error bars include the uncertainty due to fluctuations of laser intensity and the uncertainty for the temperature of the atom clouds. We note that the data are well fitted by a linear function. It is also noted that the value of β obtained from the fitting is consistent with our estimation of the Franck-Condon factor of the bound-bound transition, which also ensures the validity of our analysis. The resonance position at $\delta_{\mathrm{LS}}=0$ gives the peak position without the light shift. For the Autler-Townes spectroscopy the light shift was basically caused by the laser L_1. When the detuning Δ was not zero, however, the laser L_2 also contributed to the light shift. The sense and magnitude of the detuning Δ could be estimated from the careful investigation of the spectral shape [26]. Similarly, the peak positions with different laser intensities for L_1 and L_2 were measured and the light shift was compensated by extrapolation of these data.

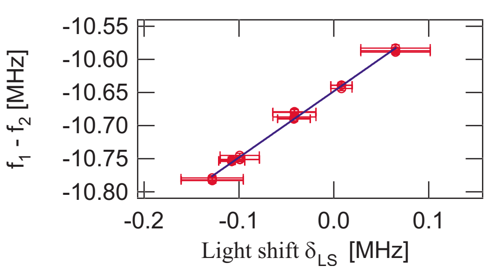

FIG. 4. (Color online) Resonance positions f_1-f_2 of the $v=1$, $J=0$ state of $^{174}\mathrm{Yb}_2$ as a function of δ_{LS}. The temperature shift is not compensated. The vertical error bars represent the uncertainty estimates for the temperature and the center frequency of the resonance. The horizontal error bars include the fluctuations of the laser intensities. The data are fitted with a linear function represented by a solid line.

The observed peak positions also suffered from the temperature shift. The temperature shift is assumed to be $a_T k_B T$, where a_T is a constant, k_B is the Boltzmann constant, and T is the temperature. The factor a_T was expected to be 3/2 [6], which was checked experimentally for $v=1$, $J=0$ state of $^{174}\mathrm{Yb}_2$ for the temperature range from 0.5 μK to 2 μK. The resonance positions with different temperatures are shown in Fig. 5. The data were fitted with a linear function represented in a solid line. The results are consistent with $\frac{3}{2}k_B T$ within 9%. We compensated the temperature shift for all the data using the $\frac{3}{2}k_B T$ dependence. The final results of the experimentally determined binding energies are listed in Table II.

The light shift produced by the trapping FORT laser beams is expected to be very small, because the relevant molecular bound states are long-range molecules which spend most of the time at long interatomic distances. The light shift of the molecule is well approximated by the sum of those of the constituent atoms, which results in a quite small light shift for the two-color PA data. Even with this expectation, here we have carefully checked the effect of the possible light shifts on the determination of the binding energies. Note that the temperature dependence shown in Fig. 5

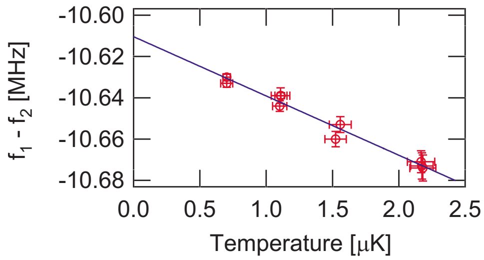

FIG. 5. (Color online) Resonance positions $f_1 - f_2$ of the $v=1$, $J=0$ state of $^{174}Yb_2$ as a function of the temperature. The light shift is not compensated. The vertical error bars represent the uncertainty estimates for the center frequency of the resonance. The horizontal error bars include the heating effect due to the irradiation of the PA lasers. The data are fitted with a linear function represented by a solid line.

was obtained by varying the intensity of the horizontal FORT beam at the final stage of the evaporative cooling to change the resultant temperature. Therefore, the data in Fig. 5 include the possible light shift. To extract the possible light shifts, first we assumed that the temperature shift is described by $\frac{3}{2}k_B T$ based on the theory of Refs. [6,27], then we subtracted the temperature shift from the obtained resonance frequencies in Fig. 5, and the subtracted data were then fitted with a function $a_I I_{\mathrm{FORT}}$, where I_{FORT} is the sum of the intensities of the horizontal and vertical FORT beams. This analysis showed that the light shifts are negligibly small well within the uncertainty in Table II. Even if the data are fitted with a function $a_T k_B T + a_I I_{\mathrm{FORT}}$, where a_T and a_I are set to be free parameters, we found that the resonance frequency obtained by the extrapolation to $T=0$ and $I_{\mathrm{FORT}}=0$ is not different from the value in Table II within the uncertainty.

We also measured E_b for the $v=1$, $J=0$ state of $^{174}Yb_2$ with the two-color PA using the strongly allowed $^1S_0 - {}^1P_1$ transition. The wavelength, linewidth, and saturation intensity of the atomic transition were 399 nm, 29 MHz, and 60 mW/cm^2, respectively. We used the $v_{e1}=157$ level of the excited $^1\Sigma_u^+$ molecular state, where v_{e1} is numbered from the dissociation limit $^1S_0 + {}^1P_1$ [19]. The resonance position of the level was -172.3 GHz from the dissociation limit. Raman spectroscopy was employed to measure the peak position. The light shift and temperature shift were also compensated. The measured E_b of 10.597(59) MHz is in excellent agreement with the values in Table II, which includes the Autler-Townes measurement with a precision of better than 20 kHz.

IV. CALCULATION AND DISCUSSION

The binding energies of the bound states as well as scattering lengths of all isotopic combinations are determined by the reduced mass and a single Born-Oppenheimer potential $V(r)$, as long as small mass-dependent adiabatic and nonadiabatic corrections to the potential are sufficiently small. The key features of the potential that determine the positions of the last few bound states are the form of the long range potential and a phase associated with the short range potential. Consequently, we assume the following simple potential form to analyze the data:

$$V(r) = -\frac{C_6}{r^6}\left(1 - \frac{\sigma^6}{r^6}\right) - \frac{C_8}{r^8} + B(r)J(J+1), \qquad (5)$$

where σ is a constant, C_8 is the van der Waals constant associated with the dipole-quadrupole interaction, and $B(r) = \hbar^2/(2\mu r^2)$ is due to molecular rotation. The first term in Eq. (5) gives the Lennard-Jones form for the potential, for which the short range form can be changed by varying σ. The C_8 term is needed to improve the quality of the fit to the data.

By solving the Schrödinger equation numerically for the eigenvalues and comparing to the measured binding ener-

TABLE II. Measured and calculated binding energies E_b for homonuclear isotopic pairs, where v and J are the vibrational and rotational quantum numbers of the ground state dimer level and v is numbered from the dissociation limit. R and AT respectively represent the Raman and Autler-Townes spectroscopic method of determining E_b.

Isotope	v	J	Method	E_b (MHz) Experiment	E_b (MHz) Theory	Difference (MHz)
^{170}Yb	1	0	R	−27.661(23)	−27.755	0.094
		2	R	−3.651(26)	−3.683	0.032
^{171}Yb	1	0	AT	−64.418(40)	−64.548	0.130
		2	AT	−31.302(50)	−31.392	0.090
^{172}Yb	1	0	AT	−123.269(26)	−123.349	0.080
		2	R	−81.786(19)	−81.879	0.093
^{173}Yb	1	0	R	−1.539(74)	−1.613	0.074
^{174}Yb	1	0	R	−10.612(38)	−10.642	0.030
	1	0	AT	−10.606(17)	−10.642	0.036
	2	0	R	−325.607(18)	−325.607	0.000
	2	2	R	−268.575(21)	−268.576	0.001
^{176}Yb	1	0	R	−70.404(11)	−70.405	0.001
	1	2	R	−37.142(13)	−37.118	−0.024

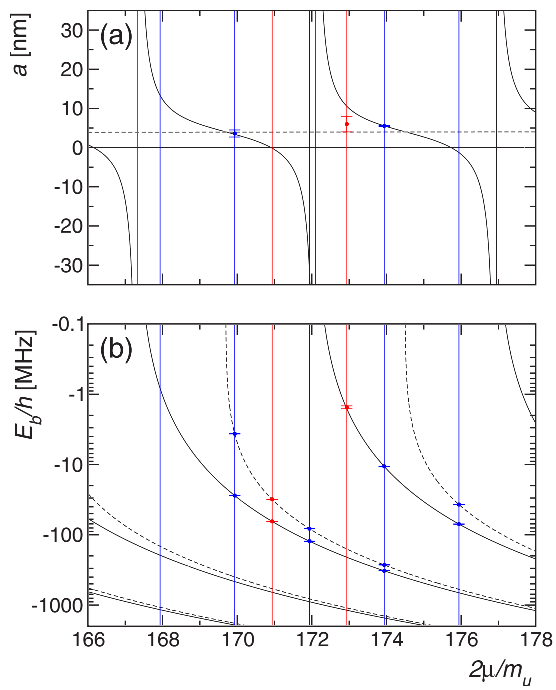

FIG. 6. (Color online) (a) Calculated scattering lengths and (b) binding energies E_b vs twice the reduced mass, 2μ, in the atomic mass unit, using the three-parameter potential energy model in Eq. (5) with the parameters given in the text. The vertical lines show the masses for the seven like-atom pairs. The solid and dashed lines in (b) show the $J=0$ and two eigenvalues, respectively. The measured values with vertical error bars are shown for the levels for which they have been measured. The measured scattering lengths of ^{170}Yb [20], ^{173}Yb [18], and ^{174}Yb [19] are also shown in (a). The horizontal dashed line in (a) shows the van der Waals length $\bar{a}$.

gies, it is possible to determine an optimum set of potential parameters. The $J=0$, $v=2$ level of $^{174}Yb_2$ and the $J=0$, $v=1$ level for $^{176}Yb_2$ were fit to determine C_6 and obtain the right number of bound states N_{174} for $^{174}Yb_2$. Then the $J=2$, $v=2$ level for $^{174}Yb_2$ was added to the fit to determine C_8 and improve the determination of C_6. The results are $C_6=1931.7\, E_h a_0^6$, $C_8=1.93\times 10^5\, E_h a_0^8$, $\sigma=9.0109362\ a_0$, and $N_{174}=72$, where $a_0\approx 0.05292$ nm and $E_h\approx 4.360\times 10^{-18}$ J. These parameters then determine without additional adjustment the binding energies of the other isotopic combinations shown in Table II and Fig. 6(b). Taking into account a lack of precise knowledge about the short range part of the potential and the magnitude of possible retardation effects and neglect of higher order dispersion energy terms, we estimate the uncertainties in C_6 and C_8 to be about 2% and 25%, respectively, or $C_6=1932(30)\, E_h a_0^6$ and $C_8=1.9(5)\times 10^5\, E_h a_0^8$. Adding a $-C_{10}/r^{10}$ van der Waals term only very slightly improved the quality of the fit, and the optimum values of C_6 and C_8 remain within the above stated uncertainties. The C_6 value is lower than a previous experimental determination of $2300(250)\, E_h a_0^6$ [19] and recent theoretical predictions of $2291.6\, E_h a_0^6$ [28], $2567.9\, E_h a_0^6$ [29], and $2062\, E_h a_0^6$ [30]. The short range form of the potential should be viewed as a pseudopotential having the right number of bound states N but not necessarily giving an accurate shape for the potential. The model well depth $D_e/h=32469$ GHz is significantly larger than *ab initio* values; see Ref [29] and references therein.

The agreement shown in Table II with a precision less than 100 kHz between the experimentally determined E_b and most of the calculated E_b values is quite impressive for such a simple model potential. The use of a single mass-independent potential with the appropriate reduced mass is thus seen as an excellent approximation for calculating the isotopic variation in binding energies. The failure to obtain a fit to the data within experimental error in all cases could be indicative of the failure of mass scaling, although it may only be due to the limitations of the simple form we assumed to represent the potential over its whole range. Adding a small mass-dependent correction on the order of 1 GHz to the well depth of the potential allows us to fit the binding energies for each isotope almost within experimental uncertainties. We see indications that the potential is deeper for heavier isotopes. Additional work is needed to see if the Yb system can be used to make quantitative tests of the accuracy and limitations of mass scaling.

When we added terms to account for relativistic retardation effects [31], the χ^2 of the overall fit did not improve, although the energies of the least bound levels improved slightly. These relativistic terms take on the form $\alpha^2 W_4/r^4$ in the physically interesting region $r\ll ƛ$, where α is the fine structure constant and $ƛ\approx 1100\, a_0$ is a characteristic length associated with a mean electronic excitation energy. The lead term in the retarded van der Waals interactions switches to $1/r^7$ behavior in the very long range region $r\gg ƛ$. Since the outer turning point of the least bound level is still only around $150\, a_0$, the $\alpha^2 W_4/r^4$ form is the appropriate form to use in looking for the magnitude of the effect. When we added a C_4/r^4 term to the potential, we find that we get a slightly better fit for the most weakly bound levels, but not a better overall fit, if we take $C_4=1.5\times 10^{-3} E_h a_0^4$, similar in magnitude to the value $0.6\times 10^{-3} E_h a_0^4$ estimated in the way proposed in Ref. [31] using the dipole polarizability and C_6 coefficient for Yb reported in Ref. [28]. Our reported model parameters and scattering lengths include the uncertainties associated with the lack of knowledge of the retardation corrections for this system. Consequently, there is a need for a theoretical evaluation of these corrections.

Given the ground state potential energy curve with the form of Eq. (5) and the parameters given above, we can calculate the *s*-wave scattering lengths for all isotopic combinations by numerically solving the Schrödinger equation with the appropriate reduced mass. These are shown in Table III and Fig. 6(a). The uncertainties reflect the uncertainties in the model parameters and the need to include retardation corrections to the potential. The value for ^{174}Yb is in excellent agreement with the value 5.53(11) nm reported in Ref. [19]. While the value for ^{170}Yb agrees with the results in Ref. [20], the value for ^{173}Yb is slightly larger than the value estimated from the thermalization experiments in Ref. [18]. However, the *s*-wave elastic cross section for ^{173}Yb decreases by about 10% between $E=0$ and the 6 μK temperature of the experiment. The experimental value could also be larger if the unknown distribution of spin populations differed from the assumption of uniformity.

Since the three-parameter model potential Eq. (5) is assumed to be common for all possible isotopic combinations,

TABLE III. Calculated s-wave scattering lengths in nm for Yb isotopic combinations. The bold numbers refer to homonuclear pairs.

	^{168}Yb	^{170}Yb	^{171}Yb	^{172}Yb	^{173}Yb	^{174}Yb	^{176}Yb
^{168}Yb	**13.33(18)**	6.19(8)	4.72(9)	3.44(10)	2.04(13)	0.13(18)	−19.0(1.6)
^{170}Yb		**3.38(11)**	1.93(13)	−0.11(19)	−4.30(36)	−27.4(2.7)	11.08(12)
^{171}Yb			**−0.15(19)**	−4.46(36)	−30.6(3.2)	22.7(7)	7.49(8)
^{172}Yb				**−31.7(3.4)**	22.1(7)	10.61(12)	5.62(8)
^{173}Yb					**10.55(11)**	7.34(8)	4.22(10)
^{174}Yb						**5.55(8)**	2.88(12)
^{176}Yb							**−1.28(23)**

the simple analytical formula Eq. (1) also holds. The predictions of this formula are completely indistinguishable from those of the numerical calculation on the scale of Fig. 6(a). The actual difference between scattering lengths calculated exactly from the model potential and those calculated from the analytical formula in Eq. (1) are below 0.03 nm for all like isotope cases except the one with the largest scattering length magnitude, ^{172}Yb, for which the difference is 0.35 nm. A similar statement applies to the mixed-isotope cases, for which most differences are below 0.03 nm.

As the reduced mass varies from 168/2 to 176/2, the scattering length varies through a complete cycle from $-\infty$ to $+\infty$. In fact, we have a rich variety of the scattering lengths from large negative values for ^{172}Yb-^{172}Yb, ^{171}Yb-^{173}Yb, ^{170}Yb-^{174}Yb, and ^{168}Yb-^{176}Yb, and almost zero for ^{171}Yb-^{171}Yb, ^{170}Yb-^{172}Yb, and ^{168}Yb-^{174}Yb, and to large positive for ^{172}Yb-^{173}Yb and ^{171}Yb-^{174}Yb. Thus the scattering length can be widely tuned by varying isotopic composition [32].

It should be noted that the observed behavior of evaporative cooling and sympathetic cooling are consistent with these scattering lengths. The efficient evaporative cooling for ^{170}Yb, ^{173}Yb, and ^{174}Yb is consistent with the large scattering lengths: 3.4 nm for ^{170}Yb, 11 nm for ^{173}Yb, and 5.6 nm for ^{174}Yb. Inefficient evaporative cooling for ^{171}Yb and ^{176}Yb is also consistent with the small scattering lengths −0.1 nm for ^{171}Yb and −1.3 nm for ^{176}Yb. On the other hand, we have successfully used sympathetic cooling to cool ^{171}Yb and ^{176}Yb with ^{174}Yb, for which the respective mixed-isotope scattering lengths are 22 nm and 2.9 nm. The extremely large value of −32 nm for ^{172}Yb would explain very rapid atom decay observed for this system, which could be due to three-body recombination.

Using the three-parameter model potential, we can also calculate the collisional properties of other partial waves at nonzero collision energies. Figure 7 shows the energy-dependent cross section for the collision of like isotopic species. The cross section can be resonantly enhanced by a shape resonance, caused by the existence of quasibound rovibrational levels supported by the centrifugal barrier. A d-wave shape resonance exists for ^{174}Yb as already pointed out in Refs. [19,22]. Our model predicts a broad peak in the collision cross section near $E/h=4.5$ MHz, or $E/k_B=220\ \mu$K, which is off-scale in Fig. 7. We found that a low energy p-wave shape resonance also exists for ^{173}Yb, giving rise to a peak in the cross section near $E/k_B=48\ \mu$K.

The s-wave contribution to the cross section becomes zero when the s-wave collisional phase shift is zero. Such a zero as a function of energy results in a Ramsauer-Townsend minimum in the cross section. This minimum is especially evident when the collision energy is so small that other partial waves make negligible contributions to the cross section, This effect occurs at very low collision energy when the scattering length has a small negative value, as for ^{171}Yb and for ^{176}Yb. Figure 7 shows the calculated cross section minima near 2 μK and 25 μK for these respective species. This effect explains why evaporative cooling is found to be inefficient for these isotopes.

V. CONCLUDING REMARKS

In conclusion, we report the accurate determination of the binding energies of the twelve least bound states in the ground molecular potentials for six Yb isotopes and the ac-

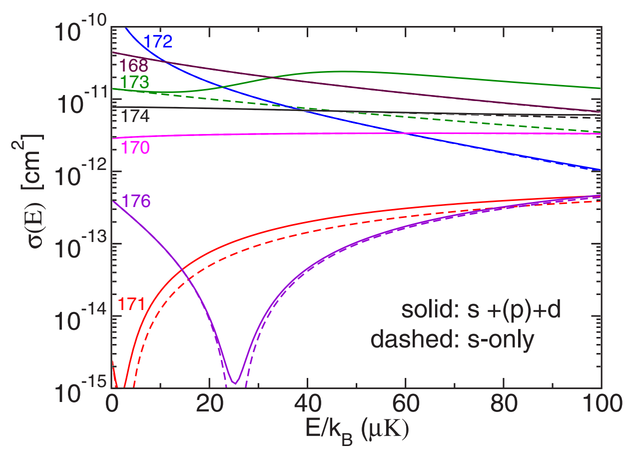

FIG. 7. (Color online) Calculated cross section $\sigma(E)$ vs collision energy E/k_B for two atoms of the same isotope. The label for each curve shows the isotopic mass number. Even mass number corresponds to identical bosons and odd mass number corresponds to two fermions with different spin projections. The dashed lines show the s-wave contribution to the total cross section. The solid lines show the contribution from s- and d-waves for the like boson cases, and the contribution from s-, p, and d-waves for the fermion case with different spin components. The $E\to 0$ cross sections are $8\pi a^2$ and $4\pi a^2$ for the respective boson and fermion cases.

curate determination of the *s*-wave scattering lengths for all possible combinations of the isotopes based on a simple three-parameter model potential. The model parameters are based on fitting a very limited set of the experimental data, making use of only three binding energies: Two bound states of $^{174}Yb_2$ and one bound state of $^{176}Yb_2$. Fitting this limited set of data allows us to reproduce the other nine binding energies with an accuracy of about 100 kHz and to determine the 28 scattering lengths for the different isotope combinations with an accuracy of about a few percent for most cases. In addition, we can calculate the energy-dependent elastic scattering due to other partial waves such as *p*- and *d*-waves. These results provide an important foundation for future research with Yb atoms on such topics as the efficiency of evaporative cooling, the stability of quantum gases and their mixtures, and clock shifts.

ACKNOWLEDGMENTS

We acknowledge S. Uetake, A. Yamaguchi, T. Fukuhara, and H. Hara for their experimental assistance. We thank M. Portier and J. Léonard for helpful comments. This work was partially supported by Grant-in-Aid for Scientific Research of JSPS (18043013, 18204035), SCOPE-S, and 21st Century COE "Center for Diversity and Universality in Physics" from MEXT of Japan. K.E. acknowledges support from JSPS. The research is also part of the program of the National Laboratory FAMO in Toruń, Poland. P.S.J. acknowledges helpful comments from E. Tiemann and partial support by the U. S. Office of Naval Research.

[1] E. R. I. Abraham, W. I. McAlexander, J. M. Gerton, R. G. Hulet, R. Côté, and A. Dalgarno, Phys. Rev. A **55**, R3299 (1997).

[2] F. A. van Abeelen and B. J. Verhaar, Phys. Rev. A **59**, 578 (1999).

[3] H. Wang, A. N. Nikolov, J. R. Ensher, P. L. Gould, E. E. Eyler, W. C. Stwalley, J. P. Burke, J. L. Bohn, C. H. Greene, E. Tiesinga, C. J. Williams, and P. S. Julienne, Phys. Lett. **62**, 052704 (2000).

[4] J. L. Roberts, N. R. Claussen, J. P. Burke, C. H. Greene, E. A. Cornell, and C. E. Wieman, Phys. Rev. Lett. **81**, 5109 (1998); S. L. Cornish, N. R. Claussen, J. L. Roberts, E. A. Cornell, and C. E. Wieman, *ibid.* **85**, 1795 (2000); P.S. Julienne, F.H. Mies, E. Tiesinga, and C.J. Williams, *ibid.* **78**, 1880 (1997).

[5] C. Chin, V. Vuletic, A. J. Kerman, and S. Chu, Phys. Rev. Lett. **85**, 2717 (2000); P. J. Leo, C. J. Williams, and P. S. Julienne, *ibid.* **85**, 2721 (2000).

[6] S. Moal, M. Portier, J. Kim, J. Dugué, U. D. Rapol, M. Leduc, and C. Cohen-Tannoudji, Phys. Rev. Lett. **96**, 023203 (2006).

[7] G. F. Gribakin and V. V. Flambaum, Phys. Rev. A **48**, 546 (1993).

[8] V. V. Flambaum, G. F. Gribakin, and C. Harabati, Phys. Rev. A **59**, 1998 (1999).

[9] C. Boisseau, E. Audouard, J. Vigué, and V. V. Flambaum, Eur. Phys. J. D **12**, 199 (2000).

[10] E. G. M. van Kempen, S. J. J. M. F. Kokkelmans, D. J. Heinzen, and B. J. Verhaar, Phys. Rev. Lett. **88**, 093201 (2002).

[11] F. Ferlaino, C. D'Errico, G. Roati, M. Zaccanti, M. Inguscio, G. Modugno, and A. Simoni, Phys. Rev. A **73**, 040702(R) (2006).

[12] P. R. Bunker and R. E. Moss, Mol. Phys. **33**, 417 (1977).

[13] L. Wolniewicz, J. Chem. Phys. **78**, 6173 (1983).

[14] C. J. Williams and P. S. Julienne, Phys. Rev. A **47**, 1524 (1993).

[15] J. Y. Seto, R. J. Le Roy, J. Vergés, and C. Amiot, J. Chem. Phys. **113**, 3067 (2000).

[16] S. Falke, E. Tiemann, and C. Lisdat, Phys. Rev. A **76**, 012724 (2007).

[17] Y. Takasu, K. Maki, K. Komori, T. Takano, K. Honda, M. Kumakura, T. Yabuzaki, and Y. Takahashi, Phys. Rev. Lett. **91**, 040404 (2003).

[18] T. Fukuhara, Y. Takasu, M. Kumakura, and Y. Takahashi, Phys. Rev. Lett. **98**, 030401 (2007).

[19] K. Enomoto, M. Kitagawa, K. Kasa, S. Tojo, and Y. Takahashi, Phys. Rev. Lett. **98**, 203201 (2007).

[20] T. Fukuhara, S. Sugawa, and Y. Takahashi, Phys. Rev. A **76**, 051604(R) (2007).

[21] M. Takamoto, F.-L. Hong, R. Higashi, and H. Katori, Nature (London) **435**, 321 (2005).

[22] S. Tojo, M. Kitagawa, K. Enomoto, Y. Kato, Y. Takasu, M. Kumakura, and Y. Takahashi, Phys. Rev. Lett. **96**, 153201 (2006).

[23] K. Honda, Y. Takasu, T. Kuwamoto, M. Kumakura, Y. Takahashi, and T. Yabuzaki, Phys. Rev. A **66**, 021401(R) (2002).

[24] T. Fukuhara, S. Sugawa, Y. Takasu, and Y. Takahashi, in *Proceedings of the International School of Physics "Enrico Fermi," Course CLXIV, Varenna*, 2006, edited by M. Inguscio, W. Ketterle, and C. Salomon (IOS Press, Amsterdam, 2007).

[25] K. Enomoto *et al.* (unpublished).

[26] J. L. Bohn and P. S. Julienne, Phys. Rev. A **54**, R4637 (1996).

[27] R. Napolitano, J. Weiner, C. J. Williams, and P. S. Julienne, Phys. Rev. Lett. **73**, 1352 (1994).

[28] X. Chu, A. Dalgarno, and G. C. Groenenboom, Phys. Rev. A **75**, 032723 (2007).

[29] A. A. Buchachenko, G. Chałasiński, and M. M. Szczęśniak, Eur. Phys. J. D **45**, 147 (2007).

[30] P. Zhang and A. Dalgarno, J. Phys. Chem. A **111**, 12471 (2007).

[31] W. J. Meath and J. O. Hirschfelder, J. Chem. Phys. **44**, 3197 (1966); **44**, 3210 (1966).

[32] Y. Takahashi, Y. Takasu, K. Komori, K. Honda, M. Kumakura, and T. Yabuzaki, in *Proceedings of the XVIIIth International Conference on Atomic Physics*, Massachusetts, 2003, edited by H. R. Sadeghpour, E. J. Heller, and D. E. Pritchard (World Scientific, New Jersey, 2002).